



HAL
open science

Progress in the development of industrial scale tungsten fibre-reinforced composite materials

J. Riesch, A. von Müller, Y. Mao, J.W. Coenen, B. Böswirth, S. Elgeti, M. Fuhr, H. Greuner, T. Höschen, K. Hunger, et al.

► To cite this version:

J. Riesch, A. von Müller, Y. Mao, J.W. Coenen, B. Böswirth, et al.. Progress in the development of industrial scale tungsten fibre-reinforced composite materials. Nuclear Materials and Energy, 2024, 38, pp.101591. 10.1016/j.nme.2024.101591 . hal-04419061

HAL Id: hal-04419061

<https://imt-mines-albi.hal.science/hal-04419061v1>

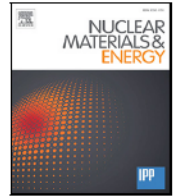
Submitted on 19 Feb 2024

HAL is a multi-disciplinary open access archive for the deposit and dissemination of scientific research documents, whether they are published or not. The documents may come from teaching and research institutions in France or abroad, or from public or private research centers.

L'archive ouverte pluridisciplinaire **HAL**, est destinée au dépôt et à la diffusion de documents scientifiques de niveau recherche, publiés ou non, émanant des établissements d'enseignement et de recherche français ou étrangers, des laboratoires publics ou privés.



Distributed under a Creative Commons Attribution 4.0 International License



Progress in the development of industrial scale tungsten fibre-reinforced composite materials

J. Riesch^{a,*}, A. von Müller^a, Y. Mao^b, J.W. Coenen^{b,c}, B. Böswirth^a, S. Elgeti^a, M. Fuhr^{a,d},
H. Greuner^a, T. Höschen^a, K. Hunger^a, P. Junghanns^a, A. Lau^b, S. Roccella^e,
L. Vanlitsenburgh^{a,f}, J.-H. You^a, Ch. Linsmeier^b, R. Neu^{a,d}

^a Max-Planck-Institut für Plasmaphysik, 85748 Garching, Germany

^b Forschungszentrum Jülich GmbH, Institut für Energie- und Klimaforschung – Plasmaphysik, 52425 Jülich, Germany

^c Department of Engineering Physics, University of Wisconsin - Madison, Madison, WI 53706, USA

^d Technische Universität München, 85748 Garching, Germany

^e ENEA Frascati Research Center, 00044 Frascati RM, Italy

^f École nationale supérieure des mines d'Albi-Carmaux, 81000 Albi, France

ARTICLE INFO

Keywords:

Tungsten
Tungsten wire
Fibre-reinforced composites
Plasma-facing components

ABSTRACT

Currently, tungsten fibre-reinforced (W_f) composites are regarded as promising materials for plasma-facing components of future magnetic confinement fusion devices. In this context, tungsten fibre-reinforced tungsten (W_f/W) is being investigated as a pseudo-ductile composite material overcoming the intrinsic brittleness of bulk tungsten while tungsten fibre-reinforced copper (W_f/Cu) is being developed as a high-strength composite heat sink material. In this contribution, we discuss the current development status and the progress that has been achieved recently with respect to characterization and upscaling of the aforementioned materials.

In cooperation with industry, upscaling of multifilamentary W yarn fabrication was demonstrated. Multilayered W fibre braids were made from such yarns and used for the manufacturing of 400 mm long medium-scale tungsten fibre-reinforced copper heat sink tubes. The maturity of short tungsten fibre-reinforced tungsten composites produced by powder metallurgy allowed the fabrication of flat tile mock-ups. Test procedure and first results of high heat flux tests are shown. Finally, we discuss the challenges and the benefits of these composites for the use in high heat flux components.

1. Introduction

A unique combination of properties such as a high melting point, low vapour pressure, low sputtering yield, and low tritium retention makes tungsten the main candidate for the plasma-facing materials in magnetic confinement fusion devices [1,2]. For example the standard design for the European DEMO¹ divertor consists of single blocks of W, so-called W monoblocks, attached to a CuCrZr cooling tube [3,4]. However, for its use in DEMO and beyond, issues regarding thermal and mechanical stability have to be resolved [5]. Especially the degradation of mechanical properties due to neutron irradiation at lower temperature (below 600–1000 °C) is of concern. This is particularly the case in regions near the heat sink, which needs to be operated below 300 °C because of the thermo-mechanical properties of the envisaged CuCrZr heat sink. Depending on the occurring stress intensity in these regions, this can be critical.

In general, the mechanical properties of tungsten are very much governed by the fabrication history and the resulting microstructure. Whereas highly deformed and fine grained tungsten, e.g. foils or wire, is ductile at room temperature [6,7], recrystallised tungsten plates can be brittle up to 1000 °C [8].

W wire is produced by severe plastic deformation in a drawing process. This leads to a fine grained microstructure with elongated grains along the drawing direction. The wire strength increases with decreasing diameter, i.e. increasing degree of deformation, and can go up to 4500 MPa [9]. Furthermore, the wire features a low ductile to brittle transition temperature (DBTT) [10] and is ductile at room temperature up to a diameter of 950 μm [11]. Potassium doping in the range of several 10 ppm is used for the stabilisation of the microstructure and thus embrittlement due to massive grain growth does only occur above 1900 °C [12].

* Corresponding author.

E-mail address: johann.riesch@ipp.mpg.de (J. Riesch).

¹ DEMO is typically the name used for the next step fusion reactor on the way to a fusion power plant.

The excellent properties of the tungsten wire are utilized in two types of composites: tungsten fibre-reinforced² copper composites (W_f/Cu) and tungsten fibre-reinforced tungsten composites (W_f/W).

Reinforcement of a copper matrix with tungsten wire has been established to increase the material strength at elevated temperature [13–16]. These W fibre-reinforced Cu (W_f/Cu) composites can exploit the extraordinary strength of drawn W fibres in combination with the high thermal conductivity of a Cu based matrix, in which the W fibres are embedded. Furthermore, this composite material offers some metallurgical flexibility, meaning that macroscopic material properties, like elasticity or the coefficient of thermal expansion, can to some extent be tailored with the fibrous preform architecture. The W-Cu material system is characterised by mutual insolubility and therefore shows no interfacial reaction. This means that W_f/Cu composite materials can be fabricated through a liquid Cu infiltration process of open porous W preforms [15]. Although, reaching high temperatures in this process (Cu melting temperature = 1085 °C [17]) the strengthening effect is maintained due to the high temperature stability of W wire [16,18]. Apart from that, the constituent materials – drawn W fibres as well as semi-finished Cu materials – are readily and industrially available at moderate cost.

Reinforcement tungsten with tungsten wire has been developed to overcome the intrinsic brittleness of tungsten below the DBTT ([1] and references therein). The use of high strength and ductile tungsten wire allows the exploitation of extrinsic toughening mechanisms and thus the increase of fracture toughness similar to ceramic fibre-reinforced ceramics. Two fabrication routes are used: chemical vapour deposition (CVD) and powder metallurgy (PM) [19,20]. The reinforcement can be continuous long fibres or randomly orientated short fibres. For PM material typically short fibre reinforcement has been used but recently progress has been achieved in long fibre reinforcement [21] which is typical for CVD material. Whereas the CVD material relies on the weak interface concept [22] in PM material the weak matrix concept is applied in addition [20,23]. Here a reduced sintering temperature leads to a reduced density and thus a reduced strength in the matrix. Growing cracks are deflected in the matrix allowing the activation of the toughening mechanisms.

In the present contribution, we discuss the current development status and the recent progress that has been made with respect to characterization and upscaling of the aforementioned materials. In particular, we present the use of braided W fibre preforms for medium-scale W_f/Cu heat sink pipes and first results of high heat flux (HHF) tests on W_f/W flat tile mock-ups with different size and thickness. Finally, we discuss the peculiarities in using composites and possible benefits when using it in high heat flux components.

2. Tungsten fibre-reinforced copper heat sinks based on braided preforms

The first step regarding the manufacturing of W_f/Cu composite materials is the fabrication of fibrous W preforms. In a first development phase, W monofilaments with diameters down to 50 μm were utilised for this purpose [15,24]. However, even thinner and thus stronger wire filaments have been used recently in the form of multifilamentary yarns. Furthermore, the application of yarns leads to an improvement regarding the textile processability due to their high flexibility. In W_f/W composites a higher reproducibility in terms of mechanical behaviour was shown by Lau et al. [25]. Different yarn architectures including enwinding, braiding, and twisting have been investigated [24,26,27]. Whereas braided yarns have been successfully

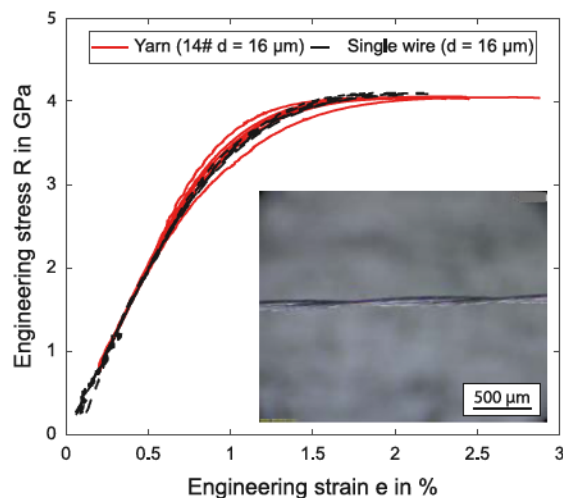


Fig. 1. Engineering stress–strain curves of a twisted yarn comprised of drawn tungsten wires with a diameter of 16 μm (red solid lines) and the pristine, as-drawn wire with a diameter of 16 μm (black dashed line) used for producing the yarn. 7 tests were performed for each material. All tensile tests were performed at room temperature. The picture in the right corner shows the yarn in detail. The yarn is built of two bundles, each consisting of seven twisted filaments (2×7), which are then wrapped around each other..

used in W_f/W composites [25], work has focused on twisted yarns recently. The main reasons are comparable low costs and scalability.

Specifically, we investigated the fabrication of a twisted W yarn comprising 14 filaments of drawn tungsten wire with a nominal diameter of 16 μm together with an industrial partner (TEC-KNIT CreativCenter für technische Textilien GmbH, Rhede, Germany). The yarn consists of two bundles with seven filaments each (2×7). At first the bundles are twisted together and then wrapped around each other to form the yarn as shown in the picture in Fig. 1. The filament wire was a potassium doped (65–75 ppm) W wire supplied by the AMS-OSRAM AG, Bruntál, Czech Republic. In tensile tests conducted at room temperature (see Fig. 1), these yarns exhibit a yield strength of 2.67 ± 0.26 GPa and a ultimate tensile strength of 4.05 ± 0.01 GPa. These values are in good agreement with the ones measured for the single filament. Details regarding the tensile tests are given in Appendix. The upscaling of the yarn fabrication was demonstrated with the industrial partners (TEC-KNIT and Haarländer GmbH in Roth, Germany) by producing a batch of about 100 km.

These yarns have subsequently been used for the preparation of preforms for heat sink pipe geometries by means of circular braiding as described in [24]. Recently, the preform fabrication has been refined to yield specimens as illustrated in Fig. 2, which shows a multilayered circular braid with a triaxial architecture produced at the DITF, Denkendorf, Germany. The braiding process was optimised in such a way that a high yarn density, i.e. a high fibre volume fraction in the later composite material, can be achieved. A high braiding angle has been desired as this leads to a preferential reinforcement and macroscopic CTE (coefficient of thermal expansion) reduction in hoop direction. Three yarn systems are used for the fabrication. Two of these are used for the primary braiding system which has a braiding angle of 75° with respect to the braiding axis. The third system introduces 24 evenly spaced yarns into the braid in an axial reinforcement direction. Details can be seen in the microscopic image of the braid in figure 2. One braided layer exhibits a thickness of approximately 0.1 mm. Hence, for a pipe with a wall thickness of 1.5 mm at least 15 braided layers are needed for the preform.

Braids as illustrated in 2 are intended to be used in liquid Cu infiltration processes for composite material fabrication. In recent years, small-scale W_f/Cu pipe specimens (outer diameter 15 mm, wall thickness 1.5 mm, length ca. 200 mm) have been fabricated according to this

² The terms wire reinforcement and fibre reinforcement are synonymous. In general the term fibre is used as soon as it is incorporated into the composite. The term tungsten fibre-reinforced composites has become established.

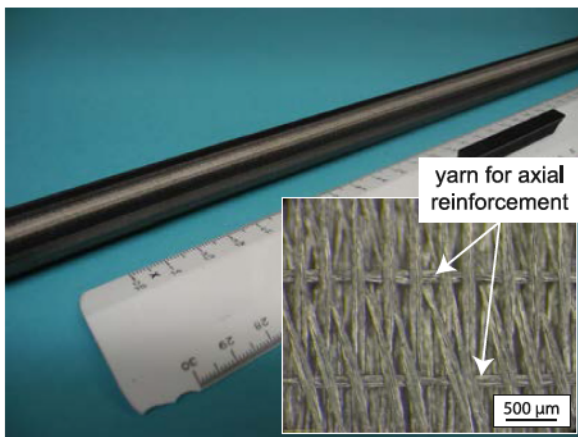


Fig. 2. Multilayered triaxial braid with axial reinforcement made of twisted W yarn ($14 \times 16 \mu\text{m}$). Magnification shows textile structure in detail. Two yarn systems are used for the braid and one for reinforcement in the axial direction.

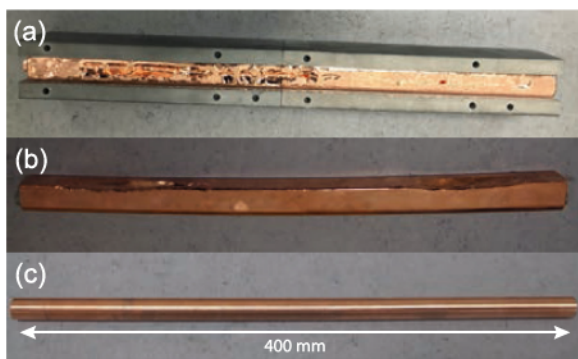


Fig. 3. Fabrication steps of medium-scale W fibre-reinforced Cu heat sink pipe specimen with a length of ca. 400 mm. (a) shows the Cu infiltrated W fibre braiding in mould after the casting. (b) shows the cast without mould. Cooling leads to deformation. In (c) the machined pipe is shown (outer diameter 15 mm, wall thickness 1.5 mm).

approach and have been applied in W monoblock-type plasma-facing component (PFC) mock-ups for high heat flux testing. Loading with conditions relevant for the European DEMO, i.e. hot water cooling conditions (inlet temperature of 130°C , inlet pressure of 40 bar, inlet velocity of 16 m s^{-1}) has been performed. The mock-ups remained fully intact even after cyclic loading up to 1000 10 s (7 s thermal equilibrium) pulses with a surface heat flux 20 MW m^{-2} [4,28].

Based on the current target design for the divertor of the European DEMO [29] the planar area and thus the straight length of a cooling pipe has to be 700 mm long. With respect to this, the fabrication of heat sink pipes with an overall length of 400 mm is conducted in cooperation with an industrial partner (Louis Renner GmbH, Bergkirchen, Germany) in a next development step. First specimens as illustrated in Fig. 3(c) have been fabricated through liquid Cu infiltration of multilayered braided preforms as illustrated in Fig. 2 in a high vacuum furnace process and subsequent machining. During the infiltration process temperatures up to approximately 1200°C have been reached. Fig. 3(a) shows an assembly of an infiltrated braided W fibre preform in a mould after the infiltration process. In Fig. 3(b) the ingot without the mould is shown. The different coefficients of thermal expansion of the involved materials lead to geometrical deviations during cooling. Manual straightening is hence required after the Cu infiltration process and before the final contour is machined. Finally, the central hole is drilled, positioned based on the outer contour.

In Fig. 4, a cross section of the pipe is shown in order to illustrate issues with the applied fabrication process. The W wire preform is well

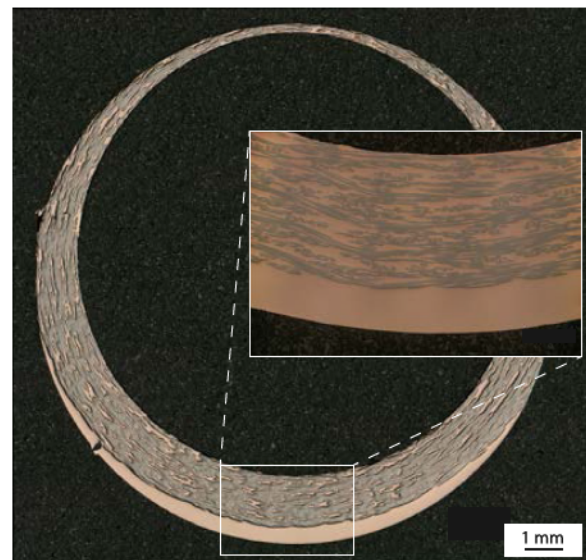


Fig. 4. Cross section of medium-scale W_t/Cu pipe. Enlargement illustrates the complete filling of W wire preform. The central hole is not centred due to geometrical variations after straightening.



Fig. 5. Medium-scale W monoblock-type PFC mock-up with W fibre-reinforced Cu heat sink pipe. 20 W monoblocks with a plasma facing size of $12 \text{ mm} \times 23 \text{ mm}$ and a height of 28 mm brazed onto a 400 mm long W_t/Cu cooling pipe. The waist in the middle of the mock-up is a photographic effect and not real.

infiltrated (see enlargement) but there is a bad coaxiality of outer and inner pipe diameters, presumably due to geometrical variations after the straightening. In the future a thicker preform in combination with state-of-the-art machining techniques like deep-hole drilling will be used to tackle this problem. Additionally we will work on optimising the furnace process to avoid deformation e.g. by using a vertical assembly infiltration instead of a horizontal one.

A medium-scale pipe as illustrated in 3 (c) was used to fabricate a PFC mock-up. W monoblocks with a pure Cu interlayer (thickness 1 mm) procured from AT&M Co., Ltd were brazed onto the pipe using 80 % Au, 20 % Cu alloy (Goldbrazo 8020, LOT-TEK GmbH) in a single step. The monoblocks had a thickness of 12 mm in the tube axis direction and a width of 23 mm in the orthogonal direction. The thickness of W on the plasma facing side has been 8 mm, with a total height of 28 mm. The brazing was performed at 970°C after degassing at 700°C . An image of such a mock-up comprising 20 W monoblocks is shown in Fig. 5.

3. Upscaling of W_t/W and high heat flux testing

Actively cooled components are subjected to large thermal gradient from the hot surface with up to 2000°C to a water cooled heat sink below 100°C [30]. Besides the stresses within the armour material, the mismatch in the coefficient of thermal expansion between this and

Table 1
Tile sizes and thicknesses of mock-ups.

No.	Tile thickness [mm]	Tile surface area [mm] × [mm]	Number of tiles
3	5	23 × 12	4
4	5	23 × 24.5	2
5	8	23 × 24.5	2
6	8	23 × 12	4

the cooling structure material results in high stresses at the interface. The design of plasma facing components is chosen to account for these stresses and keep them below the material limits to avoid the risk of failure. At the moment mono blocks with a plasma facing area of 12 mm by 23 mm are foreseen for the European DEMO [29]. However, the reduction in size comes with more complexity/effort in design and assembling e.g. to avoid the occurrence of leading edges. The high fracture toughness in W_f/W composites could allow to use larger tile sizes. Flat tile mock-ups featuring a similar and twice the plasma facing surface of the DEMO design were prepared with two different thicknesses and tested in high heat flux loading. The aim of these tests has been to evaluate the macroscopic behaviour rather than the microscopic changes which have been evaluated before.

The tiles were made from short fibre-reinforced W_f/W -composites produced by powder metallurgy. The porous matrix concept as described in [23] was used. The raw materials were short potassium doped W fibres (2.4 mm in length, 0.15 mm in diameter, 60-75 ppm potassium) and W powders with 5 μ m average particle size. At first, the short fibres were mixed with the powders with 40 % fibre mass fraction. Then the mixture was filled into a graphite sintering mould. The mould inner diameter was 105 mm. To reduce carbon contamination a 0.5 mm thick Molybdenum foil was used on top and bottom. The consolidation process was performed with a field assisted sintering facility (Sinterland Inc.). The sintering parameters were 1400 °C holding temperature (measured in mould), 100 °C min⁻¹ heating rate, 30 MPa compression and 8 min holding time at a pressure of 0.1 mbar. Sintering resulted in a disc with a diameter of 105 mm and a thickness of 30 mm. The overall relative density has been determined to be ~ 80 % based on weight and geometry. The flat tiles were cut out of the sample using electro discharge machining (EDM). In addition tiles from a forged tungsten bar were used as reference material and also cut by EDM. After cutting, the surface of the tiles was ground to remove the erosion layer (about 0.1 mm removal) and then cleaned with ethanol in an ultrasonic bath.

The W_f/W and the pure tungsten tiles were brazed on CuCrZr cooling structures using an Ag alloy (28.0 Cu, 2.0 Ge, 0.3 Ni). The brazing parameters were 840 °C for 10 min at a pressure of 1×10^{-5} mbar. After brazing the surface of each specimen was ground with SiC paper of grit P240, P320, P600, P1200, P2500 and P4000. Subsequently, the surface was polished with Al₂O₃ suspension 1 μ m grit for 5 h on a vibratory polisher. Finally, it was polished with colloidal silica 0.04 μ m for 36 h on the vibratory polisher. An overview of tile sizes and thicknesses is given in Table 1 the final mock-ups are shown in Fig. 6. To reduce bending during HHF loading a steel bar (thickness 11.3 mm) was attached on the bottom of the cooling structure using a dovetail connection. Only visual inspection was carried out for qualification.

HFF tests were performed in the GLADIS device at the Max Planck Institute for Plasma Physics in Garching, Germany. GLADIS allows a homogeneous heating of actively cooled components by H neutrals (details in [31]). The tests were performed in two steps: screening to a dedicated load and cyclic loading at the foreseen steady state power density. The inlet temperature of the cooling water was 15 °C with an inlet pressure of 17 bar and an inlet velocity of 12 m s⁻¹. During screening the samples were stepwise tested with an increasing incident heat flux up to 12 MW m⁻² except for mock-up #5 which already reached very high surface temperatures at 10 MW m⁻². The loading time for each step was 10 s to reach the thermal equilibrium safely. For cyclic loading

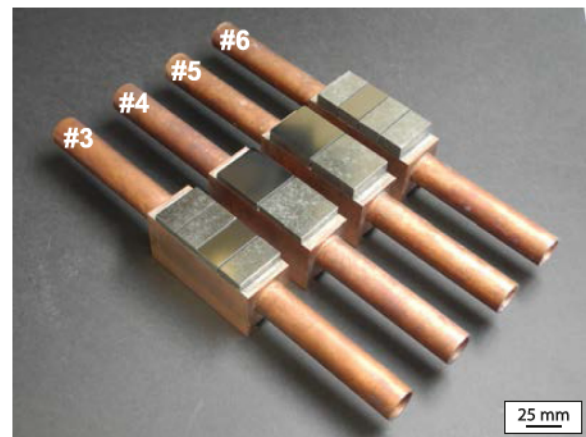


Fig. 6. Mock-ups consisting of a CuCrZr cooling structure equipped with W_f/W and W (shiny) tiles.

100 pulses with 10 MW m⁻² and 10 s loading time, have been performed. Depending on the results of this cyclic loading a successive loading step with increased heat flux was performed. Here the same procedure was performed (screening followed by 100 cycles at maximum load). During testing the surface of the tiles has been monitored using digital (CCD³) and infrared (IR) cameras. The surface temperature was measured using one colour and two colour pyrometers. Prior and after HHF loading the surface of the tiles was photographed and investigated using optical and electron microscopy. The surface roughness was determined using laser scanning microscopy and digital microscopy.

The results of the different maximum temperatures obtained for each mock-up during cycling are shown in Table 2. An increase in temperature typically corresponds to an occurrence of damage in the component. It should be noted that the existing scatter in operating parameters also leads to a scatter in surface temperature. If this increase is not evenly distributed over the entire tile, but only locally limited, these regions are called hot spots. Cyclic loading at 10 MW m⁻² was possible for all mock-ups besides #5 which already reached a surface temperature of 2500 °C during screening. After this first cycling only mock-up #3 showed no signs of degradation. Mock-up #4 showed two hot spots at the edges of the W_f/W tile. For mock-up #6 two W_f/W tiles showed degradation and were shielded from the beam using an cooled scrapper for the next loading step of 15 MW m⁻² (screening) and 12 MW m⁻² (cyclic) respectively. A similar behaviour occurred after cyclic loading of #3 at 12 MW m⁻². Thus for this mock-up only one W_f/W tile and the neighbouring W tile were loaded at 15 MW m⁻² (both screening and cyclic) at which a significant increase in surface temperature was observed during cycling. The W reference tiles had a lower surface temperature compared to the W_f/W tiles due to their higher thermal conductivity and showed no sign of degradation during loading. In summary mock-up #3 which features the smallest tiles performed the best. The larger the tiles (plasma facing surface) the larger the stress caused by the thermal expansion mismatch between the tile and the cooling structure. However, this size effect could also hint to a defect controlled behaviour and thus the influence of material homogeneity.

Detailed post examination is ongoing and in the following already available results focusing on mock-up #3 are discussed to illustrate the procedure of analysis. In a first step surface pictures before and after loading have been compared to find features leading to the occurrence of hot spots. Already before loading most of the tiles show surface cracks. These cracks are accentuated and new cracks are formed during

³ The image sensor of the camera is a charged-coupled device (CCD)

Table 2
Maximum temperature on W_f/W tiles at cyclic loading. The slight decrease in temperature between the first and last cycle in the second loading of the mock-up #3 has been caused by the scatter in operating parameters.

No.	T_{max}	T_{max}	T_{max}	T_{max}	T_{max}	T_{max}
	10 MW m ⁻²	10 MW m ⁻²	12 MW m ⁻²	12 MW m ⁻²	15 MW m ⁻²	15 MW m ⁻²
	1st cycle	100th cycle	1st cycle	100th cycle	1st cycle	100th cycle
	[°C]	[°C]	[°C]	[°C]	[°C]	[°C]
3	1140	1090	1780	1700	1970	2220
4	1180	1250				
5			no cycling — surface temperature at screening already 2580 °C			
6	1890	1950	1867	1960		

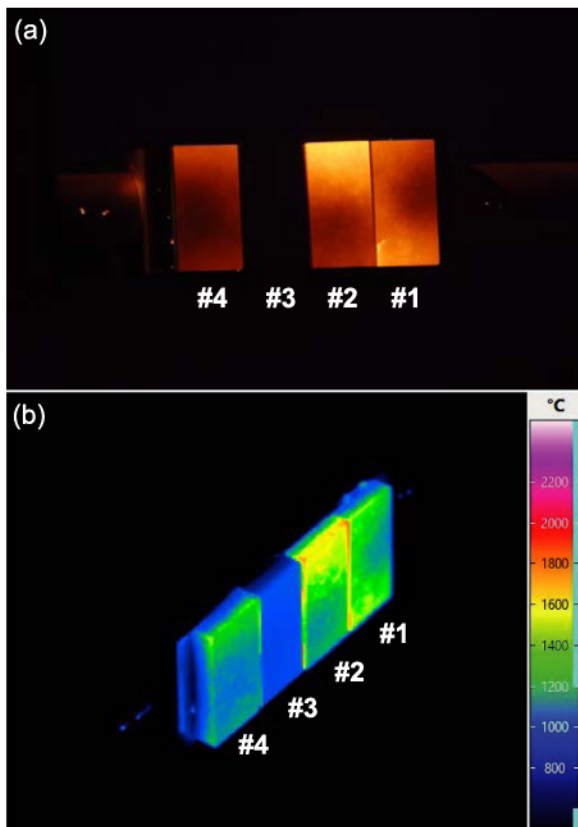


Fig. 7. Optical (a) and infrared (b) image of mock-up #3 at cycle 100 for a loading of 12 MW m⁻². The mock-up is equipped with 4 tiles with a size of 23 mm × 12 mm and a thickness of 5 mm. Hot spots are visible on the edges of tile #1 and #2. Due to the higher thermal conductivity the pure tungsten tile #3 is cooler. Tile #4 shows no noticeable features.

the tests. This happens at all three loading levels. Crack deflection on surface fibres has been observed. The surface cracks are not linked to hot spots first observed during the cyclic loading at 12 MW m⁻². Here, two tiles show hot spots at which the temperature rose above 1700 °C (see Fig. 7). As mentioned above, tile #1 and #2 were shielded when loading the mock up to 15 MW m⁻². During cycling the whole tile #4 got hotter, more pronounced at the edges.

In a next step, side views are used to evaluate the reasons for degradation/failure. The side view shown in Fig. 8 reveals several features which might be linked to the hot spots. There seems to be a gap present between the tungsten and copper in tile #3 and #4. While tile #4 shows a hot spot tile #3 did not show any sign of degradation. Further examination is needed to assess whether debonding is present or not. There are cracks visible in tile #2 and #4 but only tile #4 showed a hot spot on this side. The W_f/W tiles show inhomogeneities regarding density (considering bright regions as dense and black regions as pores) and fibre distribution. Especially tile #1 which showed a hot spot on this side is very inhomogeneous. At this point a conclusion about the

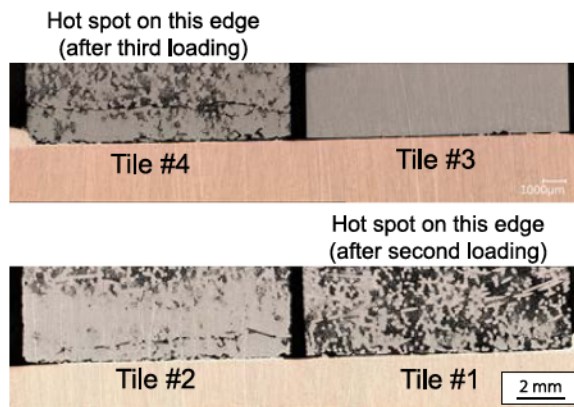


Fig. 8. Side view of mock-up #3. Several features are visible. Tile #4 and #2 show large cracks. Overall the material looks very inhomogeneous which is very obvious for tile #1. In this image tile #4 and #3 seems to be debonded from the cooper structure. These features are not linked to the hot spots during HHF loading which occurred on tile #4 and tile #1.

governing feature is not possible. The next step will be to section the tiles and investigate the distribution of the features within the volume. Electron microscopy will be used to get an better idea of the interfaces between the tiles and the cooling structure and comparison to as-fabricated material will be used to understand the occurrence of volume cracks. A similar procedure will be performed for the other mock-ups in order to draw a conclusive picture of the governing mechanism.

4. W_f Composites for high heat flux components

Both W_f/Cu and W_f/W are new concepts for materials used in the standard design for the European DEMO divertor (see chapter 1 for details). They offer interesting material property combinations which could be a driving force for new designs and functionality. As composites can have tailor-made properties, designs using composite materials are often driven by the requirements of a specific application. Chawla [32] summarizes this in the statement that you should start with the function and not the material. This principle is very well applicable for the here presented tungsten fibre-reinforced composites.

In the case of W_f/Cu , the development started with the aim of increasing the strength of the heat sink tube material at elevated temperatures due to expected issues with thermal softening above 400 °C [33]. Considering this, reinforcement in hoop direction using a braided fibrous preform was the starting point. In addition, the fabrication technologies were chosen that are compatible with the cylindrical geometry. To this end, a W fibre-reinforced Cu tube could be processed successfully showing the desired higher strength. Therefore the material is considered as an alternative concept for the European DEMO reactor [4] leading to the activities of upscaling presented in Section 2.

On the other hand the development of W_f/W started when tungsten was still considered as a structural material (see e.g. [34] for an overview). For structural applications fracture toughness and strength

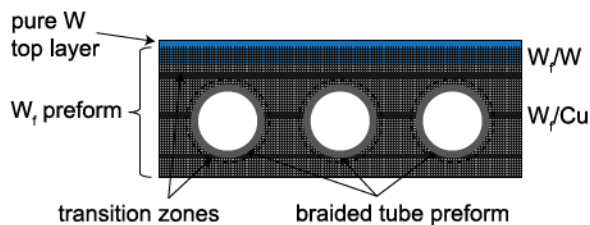


Fig. 9. Schematic drawing of mock-up made of W fibre-reinforced copper and tungsten featuring a joint fibre preform. In a real component many details need to be clarified e.g. whether a braided tube is used or a pure W layer needs to be on the top. Also the transitions between the individual composite structures need to be engineered.

are significant. Because of this the development was focusing on increasing the fracture toughness below the ductile to brittle transition temperature and mitigate concerns of operational embrittlement (see references in Section 1). The focus was on model systems to provide the proof of principle both for the toughening and fabrication technology. To this end it could be shown that the composites could be readily processed and provide a significant increase in toughness compared to bulk tungsten.

The current work is concerned with scaling up production and ensuring material quality in the process. Homogeneous material could be produced on small scale [35,36]. On a larger scale, issues are different for CVD and PM material. Whereas CVD material features internal interfaces and few large pores due to the layered fabrication process [37] PM material can still be quite inhomogeneous as can be seen in Fig. 8. Although, porosity in W_f/W produced by PM seems to have little effect on D retention due to the open pore structure [38] the material integrity has to be sufficient.

However, a recent fracture mechanics-based study showed that for the current design of the European DEMO divertor target a strongly reduced toughness and even initiated cracks in the W blocks would pose little risk on the overall structural integrity and performance. Thus embrittlement during operation was accepted in the current design accordingly [39]. Although this design that is optimized for bulk tungsten does presently not seem to require the inclusion of W_f/W composites, the potential utilization of W_f/W should still be considered for future nuclear fusion devices with regard to design flexibility and risk mitigation. This is especially true with respect to synergistic effects in a working fusion environment and anticipated long time operation. With respect to the above discussion, the approach should not be attempting to replace W one-to-one with W_f/W in the current design but to answer the question where the specific properties of W_f/W might be useful.

The use of a joint W_f preform for W and Cu based composites could improve the strength of the joint between a W armour and a copper heat sink and thus allow for flat tile concepts and larger tiles. This could be realized using a combination of liquid Cu infiltration and tungsten matrix production by CVD. In Fig. 9 a schematic drawing of a structure featuring such a joint preform is shown. The increased resistance to failure would help to suppress critical stresses within the armour material caused by the larger size. Furthermore, it could also open the path to allow tungsten to take on a structural function again. Flat tile concepts would allow to reduce the amount of W thereby reducing costs and could give more design flexibility especially with respect to cooling concepts. Tiles featuring a larger plasma facing area could reduce the complexity in installation avoiding the number of potential leading edges and allowing a more shallow chamfering. However, as flat tile concepts theoretically run the risk of complete delamination of tiles, special attention has to be paid to the joint of tile and heat sink.

W wire used in the composites was designed for the lightning industry [40] and thus for high temperature application. Due to doping with potassium in combination with the intense plastic deformation

during processing the microstructure is stabilized up to high temperature. Extensive grain growth leading to a deterioration of the good mechanical properties is only observed at a temperature above 2000 °C which is almost 600 °C more than typically reported for tungsten [12]. This could allow to increase the allowed temperature in regions where recrystallisation and embrittlement is not allowed/desired. To ensure the desired properties a thorough design of the fibre matrix interface is crucial (see [41]). Depending on W armour thickness the surface temperature can rise well above 2000 °C at 20 MW m⁻² [29]. In regions where this temperature is reached recrystallisation and extensive grain growth will also occur for W wire. The effect of these areas on the component behaviour needs to be investigated.

The change of material properties due to neutron irradiation will be critical for future fusion devices (see also chapter 1). The principle of toughening used in W_f/W is also working for brittle composite components as in ceramic fibre reinforced ceramics [42] and thus could be resilient for embrittlement due to irradiation. The reduced strength in embrittled W wire [43] has to be taken into account. In addition, it was shown that W wire is in general less prone to this embrittlement. This was done for the single wire in ion irradiation experiments [44] and when used in composites [45] exposed to fission irradiation. Recently, a device has been commissioned which allows to perform in situ mechanical testing of W wire samples while being irradiated with MeV energy ions (e.g. helium, protons, tungsten) from a 3 MV tandem accelerator or keV ions from a plasma source (e.g. helium, deuterium). This device will allow to get insight into the synergistic effects expected in a future fusion reactor and thus provide a solid basis for the further use of W wire.

5. Summary and conclusion

Textile processes for W wire already reached industrialisation e.g. large scale W yarn fabrication and are now used for braided preforms for tungsten fibre-reinforced copper composites cooling pipes. Upscaling and industrialisation of pipe fabrication is ongoing but a challenging process. Maturity is reached for short tungsten fibre-reinforced tungsten composites produced by powder metallurgy. This allowed the fabrication of mock-ups with larger tiles (compared to current design approaches) to investigate the effect of increased fracture toughness. High heat flux tests have been performed and show a large spread in results depending on size and thickness. Detailed evaluation is ongoing to determine governing mechanisms e.g. the role of observed material inhomogeneities.

To make use of fibre-reinforced composites in high heat flux components the composites have to be designed according to a function. A good example is the excellent performance of tungsten fibre-reinforced copper for cooling pipes. This has still to be proven for tungsten fibre-reinforced tungsten whereas there is great potential specifically in the improvement of irradiation resilience. Taking these aspects into account the next step in development of tungsten fibre-reinforced composites has to be in close cooperation with industry regarding the question of upscaling and plasma facing component designers with respect to the integration in HHF components in general.

CRedit authorship contribution statement

J. Riesch: Conceptualization, Formal analysis, Methodology, Supervision, Writing – original draft, Project administration, Visualization. **A. von Müller:** Conceptualization, Formal analysis, Methodology, Project administration, Supervision, Writing – review & editing. **Y. Mao:** Conceptualization, Data curation, Formal analysis, Writing – review & editing. **J.W. Coenen:** Conceptualization, Supervision, Writing – review & editing. **B. Böswirth:** Data curation, Formal analysis, Investigation, Writing – review & editing. **S. Elgeti:** Data curation, Formal analysis, Visualization, Writing – review & editing. **M. Fuhr:** Data curation, Formal analysis, Writing – review & editing. **H. Greuner:** Formal

analysis, Methodology, Writing – review & editing. **T. Höschchen:** Formal analysis, Methodology, Writing – review & editing. **K. Hunger:** Data curation, Formal analysis, Visualization, Writing – review & editing. **P. Junghanns:** Data curation, Formal analysis, Investigation, Writing – review & editing. **A. Lau:** Methodology, Writing – review & editing. **S. Roccella:** Resources, Writing – review & editing. **L. Vanlitsenburgh:** Formal analysis, Investigation, Visualization, Writing – review & editing. **J.-H. You:** Methodology, Validation, Writing – review & editing. **Ch. Linsmeier:** Funding acquisition, Project administration, Writing – review & editing. **R. Neu:** Funding acquisition, Project administration, Writing – review & editing.

Declaration of competing interest

The authors declare that they have no known competing financial interests or personal relationships that could have appeared to influence the work reported in this paper.

Data availability

Data will be made available on request.

Acknowledgements

We want to acknowledge the contributions from our industrial partners. The AMS-OSRAM AG in Bruntál, Czech Republic, for supplying the wire, the TEC-KNIT Creativ Center für technische Textilien GmbH, in Rhede, Germany, and the Haarländer GmbH in Roth, Germany for the collaboration in yarn fabrication, the DITF (Deutsche Institute für Textil- und Faserforschung) in Denkendorf, Germany, for textile processing and the Louis Renner GmbH in Bergkirchen, Germany, for their work in the production of W_f/Cu composites. Finally, we want to thank the Hefei University of technology for the fabrication of W_f/W raw materials.

This work has been carried out within the framework of the EUROfusion Consortium, funded by the European Union via the Euratom Research and Training Programme (Grant Agreement No 101052200 – EUROfusion). Views and opinions expressed are however those of the author(s) only and do not necessarily reflect those of the European Union or the European Commission. Neither the European Union nor the European Commission can be held responsible for them.

Appendix. Tensile testing of twisted W yarns

The mechanical properties of yarns were characterised using uniaxial tensile tests at room temperature. The instruments and methods outlined in [9,11] were used: Tensile tests on wire samples with a free length of 30 mm were tested using a TIRAtest[®] 2820 universal testing machine equipped with a 20 N load cell. The sample ends clamped at the upper and lower cross-head were covered in cured epoxy glue (UHU[®] Endfest 300) in order to ensure that the fracture of the samples occurred within the free gauge length. The tests were performed with a constant cross-head velocity of $5 \mu\text{m s}^{-1}$. During the mechanical tests, the sample surface was recorded using a camera system consisting of a CMOS image sensor (Toshiba[®] DU657M) and a telecentric lens (Opto Engineering[®] TC110-08/C). Using a custom digital image correlation algorithm written in LabView[®], the relative elongation of certain regions of the sample and thus the local strain ϵ is calculated. The elastic strain measured in each test was adjusted in a way that the slope in the elastic region matches the Young's modulus of tungsten at room temperature (410 GPa [46]).

References

- [1] J.W. Coenen, Fusion materials development at Forschungszentrum Jülich, Adv. Eng. Mater. 22 (6) (2020) <http://dx.doi.org/10.1002/adem.201901376>.
- [2] V. Philipps, Tungsten as material for plasma-facing components in fusion devices, J. Nucl. Mater. 415 (1) (2011) S2–S9, <http://dx.doi.org/10.1016/j.jnucmat.2011.01.110>.
- [3] H. Greuner, B. Böswirth, K. Hunger, A. Khan, T.R. Barrett, F. Gally, M. Richou, E. Visca, A.V. Müller, J.H. You, Assessment of the high heat flux performance of European DEMO divertor mock-ups, Phys. Scr. T171 (2020) 014003, <http://dx.doi.org/10.1088/1402-4896/ab3681>.
- [4] J.H. You, E. Visca, T. Barrett, B. Böswirth, F. Crescenzi, F. Domptail, G. Dose, M. Fursdon, F. Gally, H. Greuner, K. Hunger, A. Lukenskas, A. Müller, M. Richou, S. Roccella, C. Vorpahl, K. Zhang, High-heat-flux technologies for the European demo divertor targets: State-of-the-art and a review of the latest testing campaign, J. Nucl. Mater. 544 (2021) 152670, <http://dx.doi.org/10.1016/j.jnucmat.2020.152670>.
- [5] G. Pintsuk, A. Hasegawa, Tungsten as a plasma-facing material, in: Comprehensive Nuclear Materials, Elsevier, 2020, pp. 19–53, <http://dx.doi.org/10.1016/B978-0-12-803581-8.11696-0>.
- [6] J. Reiser, M. Rieth, A. Möslang, B. Dafferner, A. Hoffmann, X. Yi, D. Armstrong, Tungsten foil laminate for structural divertor applications – Tensile test properties of tungsten foil, J. Nucl. Mater. 434 (1–3) (2013) 357–366, <http://dx.doi.org/10.1016/j.jnucmat.2012.12.003>.
- [7] P. Zhao, J. Riesch, T. Höschchen, J. Almanstötter, M. Balden, J.W. Coenen, R. Himmel, W. Pantleon, U. von Toussaint, R. Neu, Microstructure, mechanical behaviour and fracture of pure tungsten wire after different heat treatments, Int. J. Refract. Met. Hard Mater. 68 (2017) 29–40, <http://dx.doi.org/10.1016/j.jrmhm.2017.06.001>.
- [8] J. Reiser, M. Rieth, B. Dafferner, A. Hoffmann, Charpy impact properties of pure tungsten plate material in as-received and recrystallized condition (1 h at 2000 °C (2273 K)), J. Nucl. Mater. 442 (1–3) (2013) S204–S207, <http://dx.doi.org/10.1016/j.jnucmat.2012.10.037>.
- [9] J. Riesch, A. Feichtmayer, M. Fuhr, J. Almanstötter, J.W. Coenen, H. Gietl, T. Höschchen, C. Linsmeier, R. Neu, Tensile behaviour of drawn tungsten wire used in tungsten fibre-reinforced tungsten composites, Phys. Scr. T170 (2017) 014032, <http://dx.doi.org/10.1088/1402-4896/aa891d>.
- [10] H. Gietl, J. Riesch, T. Höschchen, M. Rieth, J.W. Coenen, R. Neu, Charpy impact tests of tungsten fiber-reinforced composite from –150 °C to 1000 °C, Mater. Lett. 311 (2022) 131526, <http://dx.doi.org/10.1016/j.matlet.2021.131526>.
- [11] M. Fuhr, T. Höschchen, J. Riesch, M. Boleininger, J. Almanstötter, W. Pantleon, R. Neu, Rate-controlling deformation mechanisms in drawn tungsten wires, Phil. Mag. (2023) 1–19, <http://dx.doi.org/10.1080/14786435.2023.2184877>.
- [12] D. Terentyev, J. Riesch, A. Dubinko, T. Khvan, E.E. Zhurkin, Fracture surfaces of tungsten wires used in fiber-reinforced plasma facing components: Effect of potassium doping and high temperature annealing, Fusion Eng. Des. 146 (2019) 991–994, <http://dx.doi.org/10.1016/j.fusengdes.2019.01.137>.
- [13] D.L. McDanel, Tungsten Fiber Reinforced Copper Matrix Composites: A Review, NASA Technical Paper 2924 ADA309283, Lewis Research Center, Cleveland, Ohio, 1989.
- [14] J.-H. You, Copper matrix composites as heat sink materials for water-cooled divertor target, Nucl. Mater. Energy 5 (2015) 7–18, <http://dx.doi.org/10.1016/j.nme.2015.10.001>.
- [15] A. Müller, D. Ewert, A. Galatanu, M. Milwich, R. Neu, J.Y. Pastor, U. Siefken, E. Tejado, J.H. You, Melt infiltrated tungsten–copper composites as advanced heat sink materials for plasma facing components of future nuclear fusion devices, Fusion Eng. Des. 124 (2017) 455–459, <http://dx.doi.org/10.1016/j.fusengdes.2017.01.042>.
- [16] A.V. Müller, M. Ilg, H. Gietl, T. Höschchen, R. Neu, G. Pintsuk, J. Riesch, U. Siefken, J.H. You, The effects of heat treatment at temperatures of 1100 °C to 1300 °C on the tensile properties of high-strength drawn tungsten fibres, Nucl. Mater. Energy 16 (2018) 163–167, <http://dx.doi.org/10.1016/j.nme.2018.06.003>.
- [17] X. Liu, X. Xiong, Copper, in: W.M. White (Ed.), Encyclopedia of Geochemistry, in: Encyclopedia of Earth Sciences Series, Springer International Publishing, Cham, 2018, pp. 303–305, http://dx.doi.org/10.1007/978-3-319-39312-4_216.
- [18] D. Terentyev, J. Riesch, S. Lebediev, T. Khvan, A. Dubinko, A. Bakaeva, Strength and deformation mechanism of tungsten wires exposed to high temperature annealing: Impact of potassium doping, Int. J. Refract. Met. Hard Mater. 76 (2018) 226–233, <http://dx.doi.org/10.1016/j.jrmhm.2018.07.002>.
- [19] L. Raumann, J.W. Coenen, J. Riesch, Y. Mao, D. Schwalenberg, H. Gietl, C. Linsmeier, O. Guillon, Improving the w coating uniformity by a COMSOL model-based cvd parameter study for denser Wf/W composites, Metals 11 (7) (2021) 1089, <http://dx.doi.org/10.3390/met11071089>.
- [20] Y. Mao, J. Coenen, S. Sistla, C. Liu, A. Terra, X. Tan, J. Riesch, T. Höschchen, Y. Wu, C. Broeckmann, C. Linsmeier, Design of tungsten fiber-reinforced tungsten composites with porous matrix, Mater. Sci. Eng. A 817 (2021) 141361, <http://dx.doi.org/10.1016/j.msea.2021.141361>.
- [21] Y. Mao, J.W. Coenen, C. Liu, A. Terra, X. Tan, J. Riesch, T. Höschchen, Y. Wu, C. Broeckmann, C. Linsmeier, Powder metallurgy produced aligned long tungsten fiber reinforced tungsten composites, J. Nucl. Eng. 3 (4) (2022) 446–452, <http://dx.doi.org/10.3390/jne3040030>.

- [22] J. Du, T. Höschel, M. Rasinski, S. Wurster, W. Grosinger, J.-H. You, Feasibility study of a tungsten wire-reinforced tungsten matrix composite with ZrOx interfacial coatings, *Compos. Sci. Technol.* 70 (10) (2010) 1482–1489, <http://dx.doi.org/10.1016/j.compscitech.2010.04.028>.
- [23] Y. Mao, J.W. Coenen, S. Sistla, X. Tan, J. Riesch, L. Raumann, D. Schwalenberg, T. Höschel, C. Chen, Y. Wu, C. Broeckmann, C. Linsmeier, Development of tungsten fiber-reinforced tungsten with a porous matrix, *Phys. Scr. T171* (2020) 014030, <http://dx.doi.org/10.1088/1402-4896/ab482e>.
- [24] H. Gietl, A.V. Müller, J.W. Coenen, M. Decius, D. Ewert, T. Höschel, P. Huber, M. Milwich, J. Riesch, R. Neu, Textile preforms for tungsten fibre-reinforced composites, *J. Compos. Mater.* 52 (28) (2018) 3875–3884, <http://dx.doi.org/10.1177/0021998318771149>.
- [25] A. Lau, J.W. Coenen, D. Schwalenberg, Y. Mao, T. Höschel, J. Riesch, L. Raumann, M. Treitz, H. Gietl, A. Terra, B. Göhls, C. Linsmeier, K. Theis-Bröhl, J. Gonzalez-Julian, Bulk tungsten fiber-reinforced tungsten (Wf/W) composites using yarn-based textile preforms, *J. Nucl. Eng.* 4 (2) (2023) 375–390, <http://dx.doi.org/10.3390/jne4020027>.
- [26] J.W. Coenen, M. Treitz, H. Gietl, P. Huber, T. Hoeschen, L. Raumann, D. Schwalenberg, Y. Mao, J. Riesch, A. Terra, C. Broeckmann, O. Guillon, C. Linsmeier, R. Neu, The use of tungsten yarns in the production for W f /W, *Phys. Scr. T171* (2020) 014061, <http://dx.doi.org/10.1088/1402-4896/ab6096>.
- [27] J.W. Coenen, P. Huber, A. Lau, L. Raumann, D. Schwalenberg, Y. Mao, J. Riesch, A. Terra, C. Linsmeier, R. Neu, Tungsten fiber reinforced tungsten (Wf/W) using yarn based textile preforms, *Phys. Scr.* 96 (12) (2021) 124063, <http://dx.doi.org/10.1088/1402-4896/ac37cf>.
- [28] A.V. Müller, B. Böswirth, V. Cerri, H. Greuner, R. Neu, U. Siefken, E. Visca, J.H. You, Application of tungsten–copper composite heat sink materials to plasma-facing component mock-ups, *Phys. Scr. T171* (T171) (2020) 014015, <http://dx.doi.org/10.1088/1402-4896/ab4142>.
- [29] J.H. You, G. Mazzone, E. Visca, H. Greuner, M. Fursdon, Y. Addab, C. Bachmann, T. Barrett, U. Bonavolontà, B. Böswirth, F.M. Castrovinci, C. Carelli, D. Coccorese, R. Coppola, F. Crescenzi, G. Di Gironimo, P.A. Di Maio, G. Di Mambro, F. Dompitall, Dongiovanni, G. Dose, D. Flammini, L. Forest, P. Frosi, F. Gallay, B.E. Ghidersa, C. Harrington, K. Hunger, V. Imbriani, M. Li, A. Lukenskas, A. Maffucci, N. Mantel, Marzullo, T. Minniti, A.V. Müller, S. Noce, M.T. Porfiri, A. Quartararo, M. Richou, S. Roccella, D. Terentyev, A. Tincani, E. Vallone, S. Ventre, R. Villari, F. Villone, C. Vorpahl, K. Zhang, Divertor of the European DEMO: Engineering and technologies for power exhaust, *Fusion Eng. Des.* 175 (2022) 113010, <http://dx.doi.org/10.1016/j.fusengdes.2022.113010>.
- [30] J. Linke, J. Du, T. Loewenhoff, G. Pintsuk, B. Spilker, I. Steudel, M. Wirtz, Challenges for plasma-facing components in nuclear fusion, *Matter Radiat. Extrem.* 4 (5) (2019) <http://dx.doi.org/10.1063/1.5090100>.
- [31] H. Greuner, B. Boeswirth, J. Boscary, P. McNeely, High heat flux facility GLADIS, *J. Nucl. Mater.* 367–370 (2007) 1444–1448, <http://dx.doi.org/10.1016/j.jnucmat.2007.04.004>.
- [32] K.K. Chawla, *Composite Materials*, Springer, New York, 2012, <http://dx.doi.org/10.1007/978-0-387-74365-3>.
- [33] J.-H. You, M. Li, K. Zhang, Structural lifetime assessment for the DEMO divertor targets: Design-by-analysis approach and outstanding issues, *Fusion Eng. Des.* 164 (2021) 112203, <http://dx.doi.org/10.1016/j.fusengdes.2020.112203>.
- [34] J.-H. You, A review on two previous divertor target concepts for DEMO: mutual impact between structural design requirements and materials performance, *Nucl. Fusion* 55 (11) (2015) 113026, <http://dx.doi.org/10.1088/0029-5515/55/11/113026>.
- [35] J. Riesch, T. Höschel, C. Linsmeier, S. Wurster, J.-H. You, Enhanced toughness and stable crack propagation in a novel tungsten fibre-reinforced tungsten composite produced by chemical vapour infiltration, *Phys. Scr. T159* (2014) 014031, <http://dx.doi.org/10.1088/0031-8949/2014/T159/014031>.
- [36] Y. Mao, J.W. Coenen, J. Riesch, S. Sistla, J. Almanstötter, B. Jasper, A. Terra, T. Höschel, H. Gietl, M. Bram, J. Gonzalez-Julian, C. Linsmeier, C. Broeckmann, Development and characterization of powder metallurgically produced discontinuous tungsten fiber reinforced tungsten composites, *Phys. Scr. T170* (2017) 014005, <http://dx.doi.org/10.1088/0031-8949/2017/T170/014005>.
- [37] D. Schwalenberg, J.W. Coenen, J. Riesch, T. Hoeschen, Y. Mao, A. Lau, H. Gietl, L. Raumann, P. Huber, C. Linsmeier, R. Neu, Large-scale tungsten fibre-reinforced tungsten and its mechanical properties, *J. Nucl. Eng.* 3 (4) (2022) 306–320, <http://dx.doi.org/10.3390/jne3040018>.
- [38] Y. Mao, J.W. Coenen, A. Terra, L. Gao, A. Kreter, M. Wirtz, C. Liu, C. Chen, J. Riesch, Y. Wu, C. Broeckmann, C. Linsmeier, Demonstrating tungsten fiber-reinforced porous-matrix tungsten composites for future fusion application, *Nucl. Fusion* 62 (10) (2022) 106029, <http://dx.doi.org/10.1088/1741-4326/ac8c55>.
- [39] K. Zhang, J.-H. You, Crack formation in the tungsten armour of divertor targets under high heat flux loads: A computational fracture mechanics study, *Fusion Eng. Des.* 184 (2022) 113305, <http://dx.doi.org/10.1016/j.fusengdes.2022.113305>.
- [40] P. Schade, 100Years of doped tungsten wire, *Int. J. Refract. Met. Hard Mater.* 28 (6) (2010) 648–660, <http://dx.doi.org/10.1016/j.ijrmhm.2010.05.003>.
- [41] U.M. Ciucani, L. Haus, H. Gietl, J. Riesch, W. Pantleon, Microstructural evolution in single tungsten fiber-reinforced tungsten composites during annealing: recrystallization and abnormal grain growth, *J. Nucl. Mater.* 543 (2021) 152579, <http://dx.doi.org/10.1016/j.jnucmat.2020.152579>.
- [42] J. Riesch, J.-Y. Buffiere, T. Höschel, M. Scheel, C. Linsmeier, J.-H. You, Crack bridging in as-fabricated and embrittled tungsten single fibre-reinforced tungsten composites shown by a novel in-situ high energy synchrotron tomography bending test, *Nucl. Mater. Energy* 15 (2018) 1–12, <http://dx.doi.org/10.1016/j.nme.2018.03.007>.
- [43] D. Terentyev, J. Riesch, S. Lebediev, A. Bakaeva, J.W. Coenen, Mechanical properties of as-fabricated and 2300 °C annealed tungsten wire tested up to 600 °C, *Int. J. Refract. Met. Hard Mater.* 66 (2017) 127–134, <http://dx.doi.org/10.1016/j.ijrmhm.2017.03.011>.
- [44] J. Riesch, A. Feichtmayer, J.W. Coenen, B. Curzadd, H. Gietl, T. Höschel, A. Manhard, T. Schwarz-Selinger, R. Neu, Irradiation effects in tungsten—From surface effects to bulk mechanical properties, *Nucl. Mater. Energy* 30 (2022) 101093, <http://dx.doi.org/10.1016/j.nme.2021.101093>.
- [45] D. Terentyev, M. Rieth, G. Pintsuk, A. von Müller, S. Antusch, A. Zinovov, A. Bakaev, K. Poleshchuk, G. Aiello, Effect of neutron irradiation on tensile properties of advanced Cu-based alloys and composites developed for fusion applications, *J. Nucl. Mater.* 584 (2023) 154587, <http://dx.doi.org/10.1016/j.jnucmat.2023.154587>.
- [46] R. Lowrie, A.M. Gonas, Single-crystal elastic properties of tungsten from 24 ° to 1800 °C, *J. Appl. Phys.* 38 (11) (1967) 4505–4509, <http://dx.doi.org/10.1063/1.1709158>.